Int. J. Multiphase Flow Vol. 10, No. 1, pp. 79–94, 1984
Printed in Great Britain.

0301-9322/84 $3.00 + .00
Pergamon/Elsevier

MOMENTUM TRANSFER IN A VERTICAL DOWN FLOW LIQUID JET EJECTOR: CASE OF SELF GAS ASPIRATION AND EMULSION FLOW

A. BEN BRAHIM, M. PRÉVOST and R. BUGAREL
Institut du Génie Chimique, Toulouse, France

(*Received* 1 *July* 1982; *in revised form* 13 *March* 1983)

Abstract—Momentum transfer in a vertical liquid jet contactor consisting of an ejector supported in a vertical column has been studied, using three different liquids as motive fluids, and air as the entrained gas.

On the basis of macroscopic momentum and energy balance, an overall loss factor is derived. Moreover, an empirical correlation is proposed to predict the mass flow rate of entrainment by the liquid jet system. Finally, an expression to predict the volumetric flow rate of the carried fluid available at a pressure higher than atmospheric, is given.

1. INTRODUCTION

From their working principles, ejectors are able to realize in a reduced enclosed space a momentum transfer between two fluids (a motive and an entrained one). The wide range of applications of steam and air ejectors is well known. During the past few years, air ejectors have been developed and applied to chemical engineering operations as entrainment and pumping of corrosive liquids, slurries, fumes and dust laden gases, which are otherwise difficult to deal with (Harris 1966; Phelps 1966; Shah 1968). Liquid jet ejectors may also be used for mass transfer, e.g. liquid–liquid extraction, gas absorption or stripping . . . , because of the possibility of creating intense mixing between the solvent and the solute.

Bonnington (1964) reported studies on the liquid jet ejector entraining solid materials. His work consisted in the design of parameters, i.e. power consumption, effects of temperature and cavitation on the system. Witte (1965) carried out studies on liquid gas multi-jet horizontal ejector and mentioned the phenomenon of mixing shock. He reported studies on the mechanical efficiency obtainable in the ejector system, with and without liquid recirculation.

Roy *et al.* (1972) have given the improved performance of a horizontal liquid jet ejector with creation of the mixing shock. Acharjee *et al.* (1975) studied a transfer of momentum in a vertical apparatus with upward flow of the two phases.

Laurent *et al.* (1980) have developed a simulation technique of an industrial apparatus (a turbulent venturi jet scrubber) by a laboratory scale model (laminar jet). They present liquid and gas mass transfer coefficients of both equipments and the interfacial exchange area in the venturi jet scrubber.

Taking into account these works, ejectors present a real interest for gas absorption. Under fixed conditions, they may create intense mixing from a pressure energy transmitted to a motive liquid. In that perspective, we have began this work by a research of operating conditions giving a liquid–gas emulsion. These conditions will be favourable for a gas absorption. A generalized empirical correlation has been deduced.

2. EXPERIMENTAL APPARATUS

The schematic diagram of the apparatus is shown in figure 1. It consists of an ejector of fluxero type (main piece of plant, figure 2); an extended parallel diffuser (1 m of length and 0.01 m of inside diameter), made of glass tube was provided between the divergent end of the ejector and a liquid–air separator. A pump permits the circulation of the liquid.

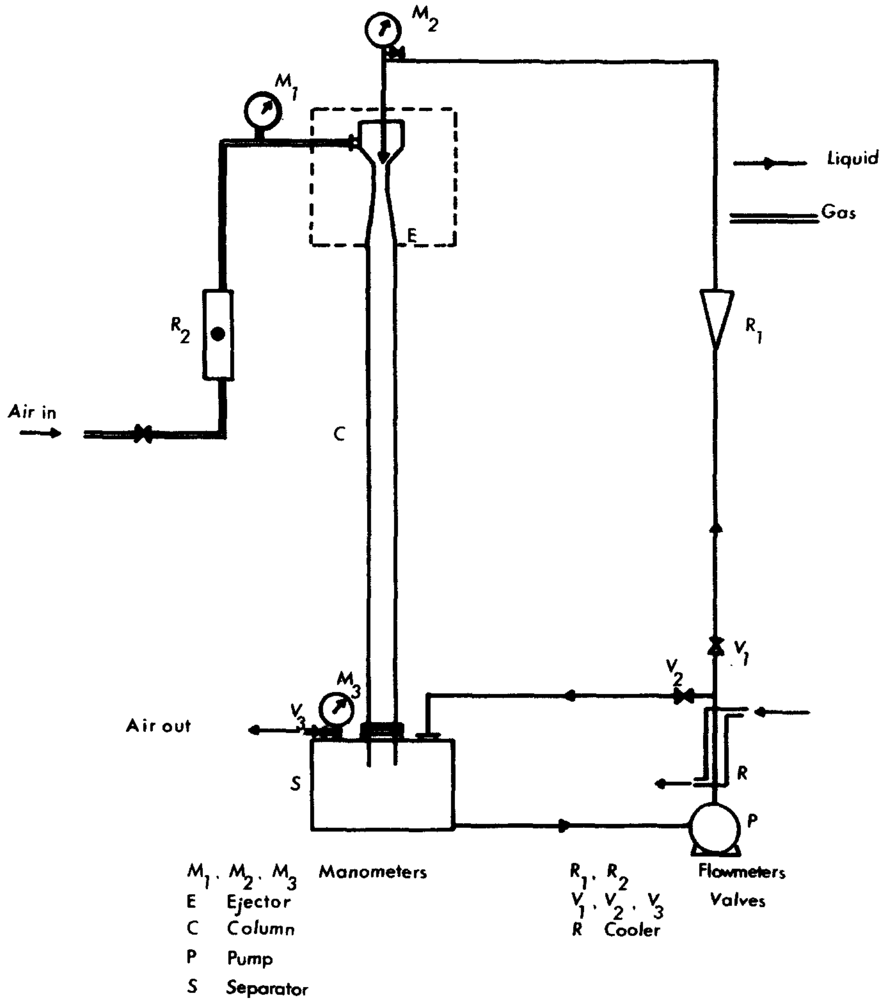

Figure 1. Schematic diagram of the apparatus.

Other accessories also exist: manometers placed at the gas entrance and on the separator, and a heat exchanger to adjust the liquid temperature at the desired level. For a given flow rate, the back pressure is controlled by means of a valve V_3 permitting to act on the flow type inside the ejector and the column.

Three motive liquids used in this study are: water, monoethylene gylcol and oil (Tellus oil 27). They cover a wide range of physical properties such as density, viscosity and surface tension in accordance with table 1. The experimental variation fields of L, V_e, P_0 and P_3 parameters are presented in table 2.

3. EXPERIMENTAL RESULTS

Generally, two types of flow (with possible combinations of the two) appeared, depending upon the operating conditions. They are:

(1) The coaxial flow of liquid and gas with trickling at the end on the inside wall of the column owing to the jet divergence. This phenomenon is frequently observed with water having low viscosity compared with the other liquids used.

(2) The formation in the mixing chamber of an emulsion involving very tiny bubbles of entrained air with the liquid. One can note that the establishment of these two types of flow mentioned by Roy et al. (1972) is related to the back pressure at the ejector.

(3) In many cases, the upper part of the column consists of coaxial flow followed by

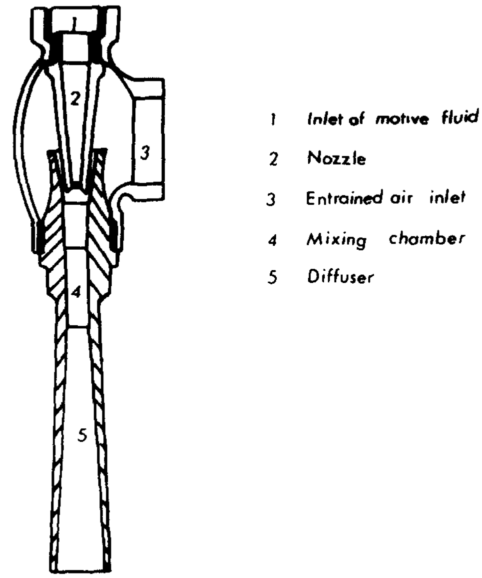

Dimension of the ejector

Fluxero commercial ejector

Material : entirely brass	5.10^{-3} m
Diameter of mixing chamber	$2.5.10^{-3}$ m
Diameter of nozzle	
Whole length (length of nozzle and diffuser)	0.12 m
Length of the throat	$17.5.10^{-3}$ m
Length of the diffuser	92.10^{-3} m
Diameter of the diffuser at the end	11.10^{-3} m

Figure 2. Scheme of the ejector.

Table 1. Physical properties of the liquids

liquids \ physico-chemical properties	density ρ_m (kg/m^3)	surface tension σ_m (N/m)	viscosity μ_m 10^3 (kg/m.s)	molecular weight 10^3 (kg/mole)	$(\frac{g \cdot u_m^4}{\rho_m \sigma_m^3})$
water	998.2	0.073	1.002	18	$25.46\ 10^{-12}$
monoethylene glycol	1102.48	0.0493	20.53	62.07	$1.32\ 10^{-5}$
oil (Tellus oil 27)	847.95	0.032	83.96	280	$1.93\ 10^{-2}$

homogeneous bubble flow at the bottom. This last phenomenon is particularly observed when the pressure difference between the input and the output of the gas reaches a certain limit, depending upon the rate of motive liquid at the nozzle tip and their physical properties.

Illustration of various types of flow is presented in figure 3. An example of typical plot showing the relationship between the entrainment rate at constant motive liquid flowrate and the separator pressure for air–water, is shown in figure 4. From this figure one should note an increase of entrained air when the homogeneous bubble flow appears. A same

Table 2. Variation field of parameters: mass flow rate of liquid L, volumic flow rate of gas V_e, P_0 and P_3, absolute pressures at sections "0" and "3"

Systems	Field of variation
Water-air	$0.06 \leq L \leq 0.113$ Kg/s $0.67 \; 10^{-5} \leq V_e \leq 13.52 \; 10^{-5}$ m^3/s $0.9 \; 10^5 \leq P_0 \leq \; 10^5$ N/m^2 $10^5 \leq P_3 \leq 1.5 \; 10^5$ N/m^2
Monoethylene-glycol-air	$0.059 \leq L \leq 0.105$ Kg/s $0.44 \; 10^{-5} \leq V_e \leq 13.56 \; 10^{-5}$ m^3/s $0.905 \; 10^5 \leq P_0 \leq \; 10^5$ N/m^2 $10^5 \leq P_3 \leq 1.38 \; 10^5$ N/m^2
Tellus oil 27-air	$0.046 \leq L \leq 0.077$ Kg/s $0.44 \; 10^{-5} \leq V_e \leq 10.56 \; 10^{-5}$ m^3/s $0.94 \; 10^5 \leq P_0 \leq 10^5$ N/m^2 $10^5 \leq P_3 \leq 1.09 \; 10^5$ N/m^2

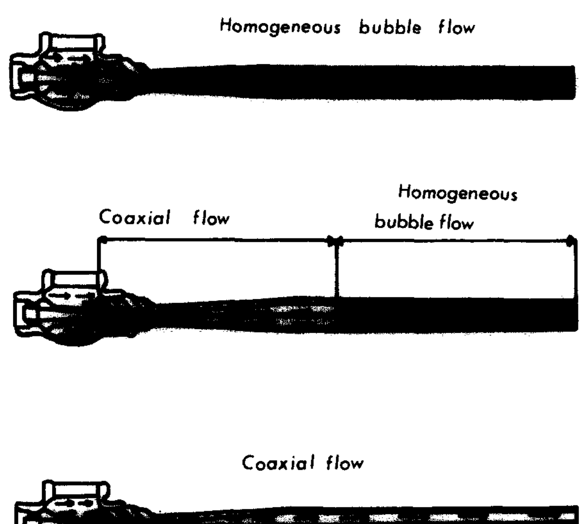

Figure 3. Sections of the contactor showing schematic flow-patterns.

phenomenon has been observed for the two other liquids. The results obtained for the three liquids permits us to draw the figure 5. It presents the location of the various flow types in function of separator pressure and liquid flow rate.

4. THEORETICAL ANALYSIS

From experimental results, macroscopic momentum and energy balances along the ejector and the column, we have tried to establish a relation permitting the Mr mass ratio prediction in the case of an homogeneous bubble flow (emulsion) favourable to mass transfer between two phases.

For convenience, the contactor has been divided into different sections 0–1, 1–2 and 2–3 as shown in figure 6. Macroscopic mechanical energy balance for control volume 0–1 and 2–3 gives:

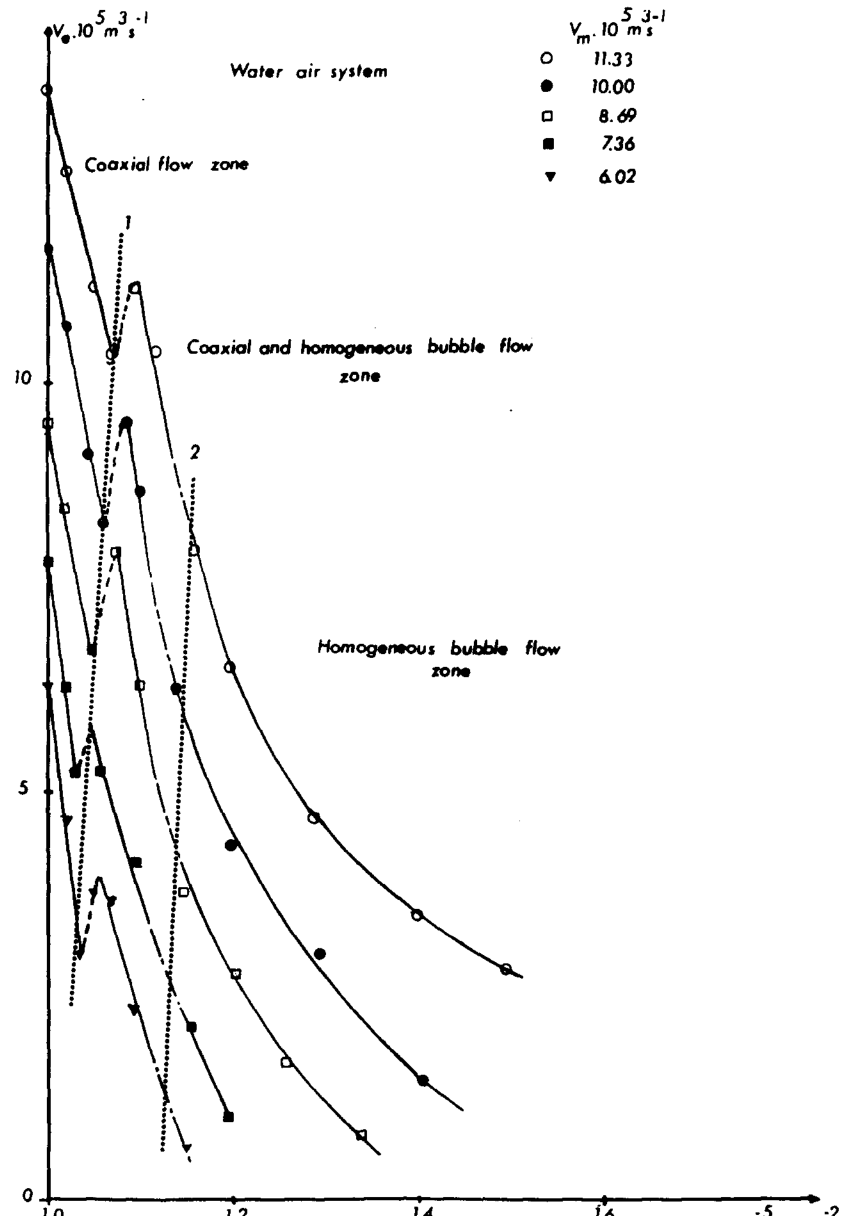

Figure 4. Effect of back pressure on entrainment rate for water–air system and for different motive liquid flowrates.

—Zone (0–1) entrained fluid: the dimensions of the ejector suggest that a variation of potential energy can be neglected (figure 2).

$$(P_1 - P_0) = \frac{1}{2}\rho_e(U_{e1}^2 - U_{e0}^2) - E_1 . \qquad [1]$$

—Zone (2–3) bubble flow: taking into account the potential energy, assuming air as a perfect gas and motive fluid as an incompressible liquid, we obtain with $U_3' \ll U_2'$:

$$V_m(P_3 - P_2) + nRT\,\mathrm{Ln}\frac{P_3}{P_2} = \frac{1}{2}(G + L)U_2'^2 + (G + L)g\Delta h - E_2' . \qquad [2]$$

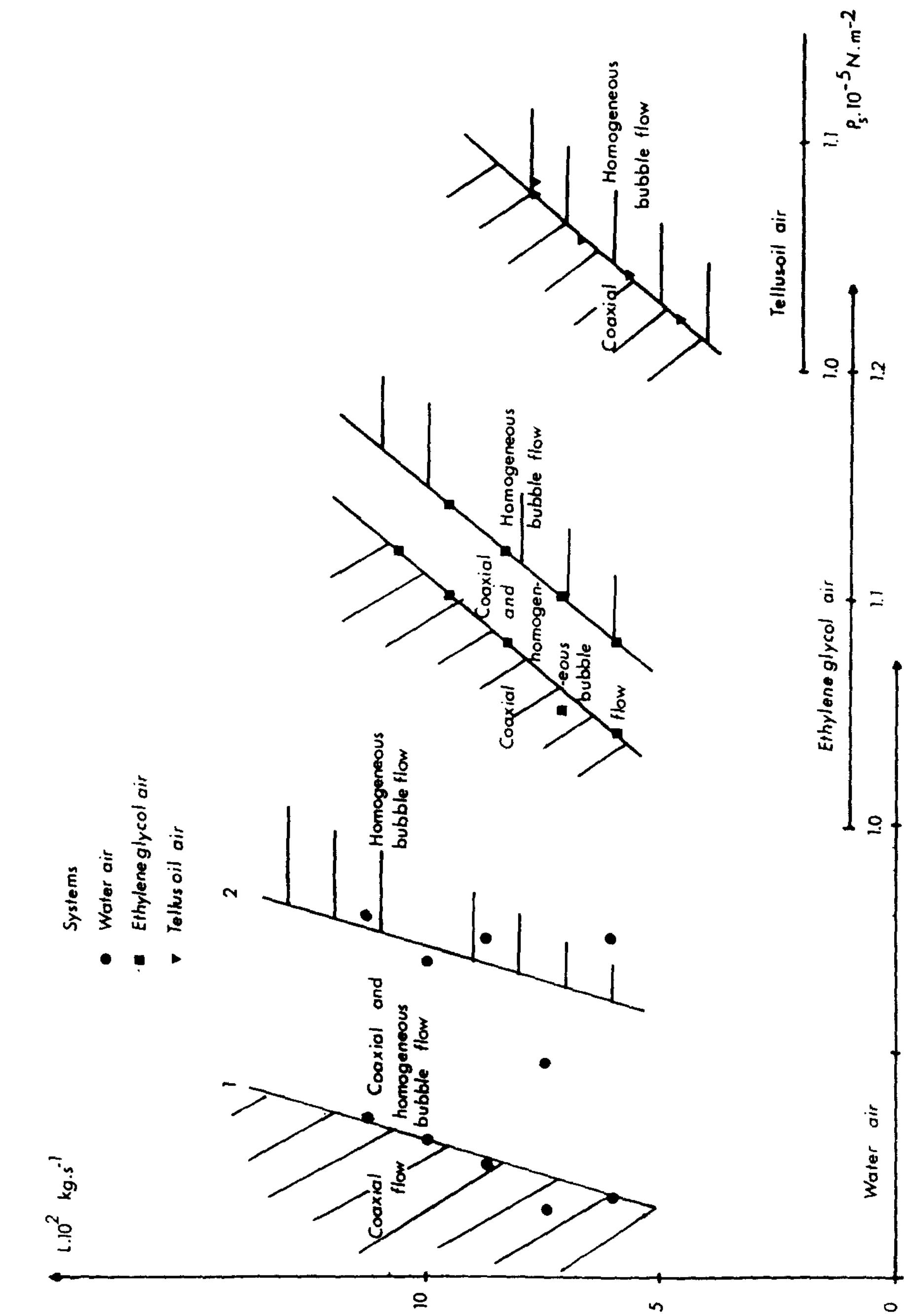

Figure 5. Change of the type of flow with back pressure.

Mass flowrates (kg/s)		Rates	
	Plane	Motive fluid	Entrained air
Motive fluid (L)	0	-	U_{e0}
Entrained air (G)	1	U_{mn}	U_{e1}
	2	U'_2	U'_2
	3	U'_3	U'_3

They correspond to well-known zones (Acharjee, Bhat, Mitra and Roy (1975), Witte (1965))

0-1 sucking of entrained air

1-2 jet flow of two phases, mixing zone

2-3 homogeneous bubble flow

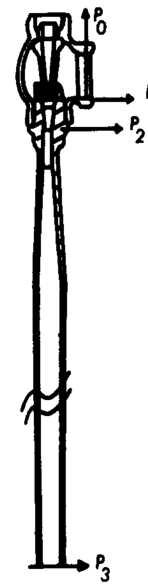

Figure 6. Scheme of the contactor.

Developing the term $nRT\,\text{Ln}\,(P_3/P_2)$, we get:

$$nRT\,\text{Ln}\,\frac{P_3}{P_2} = nRT\,\text{Ln}\left(1 + \frac{P_3 - P_2}{P_2}\right) = nRT\left(\frac{P_3 - P_2}{P_2} - \frac{(P_3 - P_2)^2}{2P_2^2} + \frac{(P_3 - P_2)^3}{3P_2^3} - \cdots\right) = \frac{nRT}{P_2}(P_3 - P_2)\left(1 - \frac{(P_3 - P_2)}{2P_2} + \frac{(P_3 - P_2)^2}{3P_2^2}\cdots\right)$$

or

$$nRT\,\text{Ln}\,\frac{P_3}{P_2} = V_{e2}(P_3 - P_2)(1 + \epsilon) \qquad [3]$$

where ϵ corresponds to

$$-\frac{(P_3 - P_2)}{2P_2} + \frac{(P_3 - P_2)^2}{3P_2^2} - \cdots$$

If the expression [3] is introduced, the relation [2] is:

$$(P_3 - P_2)[V_{m2} + V_{e2}(1 + \epsilon)] = \frac{1}{2}(L + G)U_2'^2 + (G + L)g\Delta h - E_2'. \qquad [4]$$

Dividing [4] by $[V_{m2} + V_{e2}(1 + \epsilon)]$, we get:

$$(P_3 - P_2) = \frac{1}{2}\rho_2' U_2'^2 + \rho_2' g\Delta h - E_2 \qquad [5]$$

where ρ_2' and E_2 are defined by:

$$\rho_2' = \frac{G + L}{V_{m2} + V_{e2}(1 + \epsilon)}$$

and

$$E_2 = \frac{E_2'}{V_{m2} + V_{e2}(1+\epsilon)}.$$

It may be mentioned that E_1 and E_2 are energy losses due to expansion, gas–liquid mixing, etc...

—Zone (1–2): a macroscopic momentum balance taking into account the F_1 force exerted by the two fluids on the solid wall (Bird et al. 1960), leads to:

$$P_2 a_2 - P_1 a_1 = (GU_{e1} + LU_{mn}) - (G+L)U_2 - F_1 \qquad [6]$$

Combining [1], [5] and [6], P_1 and P_2 are eliminated and we get[7]:

$$\left(P_3 - P_0\frac{a_1}{a_2}\right) = \frac{1}{2}\frac{a_1}{a_2}\rho_e(U_{e0}^2 - U_{e1}^2) + \frac{1}{2}\rho_2' U_2'^2 + \rho_2' g\Delta h$$
$$+ \frac{1}{a_2}[(GU_{e1} + LU_{mn}) - (G+L)U_2']$$
$$-\left(E_2 + E_1\frac{a_1}{a_2} + \frac{F_1}{a_2}\right). \qquad [7]$$

Grouping all these energy losses and representing them as a function of the kinetic energy of the jet, i.e. $\frac{1}{2}K'' \rho_m U_{mn}^2$ and substituting the following terms in [7]:

$$\mathrm{Ar} = \frac{a_2}{a_n} \qquad M_r = \frac{G}{L}$$

$$\mathrm{Ar}' = \frac{a_1}{a_n} \qquad \rho_r = \frac{\rho_m}{\rho_e}$$

$$\mathrm{Fr} = \frac{g\Delta h}{U_{mn}^2} \qquad \rho_2' = \frac{G(G+L)}{\dfrac{G}{\rho_e}(1+\epsilon) + \dfrac{L}{\rho_m}}$$

$$U_{e0} = \frac{G}{\rho_e a_0} \qquad \beta' = \frac{P_3 - P_0\dfrac{a_1}{a_2}}{\dfrac{1}{2}\rho_m U_{mn}^2}$$

$$U_{mn} = \frac{L\,\mathrm{Ar}}{\rho_m a_2} \qquad \gamma = \frac{a_2}{a_0}$$

and then solving, we get:

$$\mathrm{Mr}^2\rho_r\left[\gamma^2\frac{\mathrm{Ar}'}{\mathrm{Ar}} + \frac{\mathrm{Ar}\,(\mathrm{Ar}'-2)}{(\mathrm{Ar}'-1)^2}\right] + 2\,\mathrm{Ar} + \frac{1+\mathrm{Mr}}{\mathrm{Mr}\,\rho_r(1+\epsilon)}$$
$$[2\,\mathrm{Ar}^2\,\mathrm{Fr} - (\mathrm{Mr}\,\rho_r(1+\epsilon) + 1^2] - (K'' + \beta')\,\mathrm{Ar}^2 = 0\,. \qquad [8]$$

Equation [8] represents an analytical expression predicting Mr for the vertical ejector using

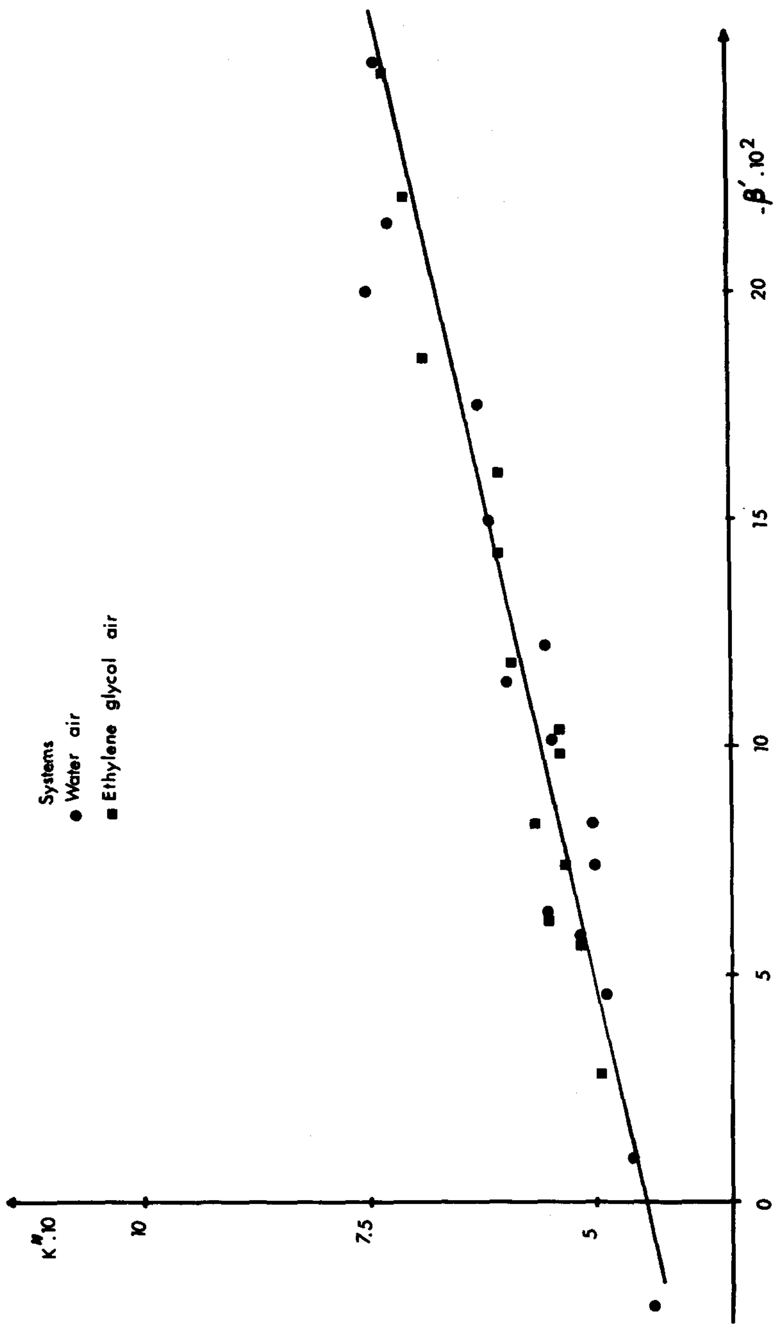

Figure 7. Relation between overall loss factor K'' and β' for different liquid air systems.

Table 3. Comparison between correlations

$K'' = a\beta' + b$ or $K'' = a\beta'' + b$

Systems	a	b	Reference	Ejector position and direction of flow
air-water air-ethylene glycol	- 1.11	0.445	this work for β'	vertical downward flow
air-water kerosene-air solution n° 1 - air at 60 % of glycerine ; solution n° 2 - air at 50 % of glycerine ; solution n° 3 - air at 35 % of glycerine	- 0.82	$\frac{1.52}{Ar^{0.95}}$	Acharjee, Bhat, Mitra and Roy (1975) for β''	vertical upward flow
the same as before	- 1.00	- 0.0123 Ar + 0.116	Bhat, Mitra and Roy (1972) for β''	horizontal

a liquid as motive fluid and the entrained air. Under the conditions of homogeneous bubble flow, experimental data obtained with water–air and ethylene–glycol–air systems are employed for the evaluation of K''. A typical plot showing a decrease of K'' with β' is presented on figure 7. It is interesting to note that the value of K'' for the two systems gives a linear relation with β' and is represented by the following equation:

$$K'' = -1.11\beta' + 0.445 .$$

The results obtained by some authors using ejectors with horizontal and upward flow formulated in the same terms are grouped in table 3. Our relation compared with that proposed by Acharjee *et al.* (1975) suggests that practically, the same relation can be used (except for β', which is β'' in their relation).

5. A DIMENSIONAL ANALYSIS

Inside the contactor, the interactions between forces are so complex, that it is difficult to write an equation which can describe perfectly the desired mixing of the two fluid streams. Hence, any theoretical correlation based on such an analysis is difficult to obtain, if a complete mixing is not achieved, and if all the terms representing the mixed fluid properties change. Therefore, a dimensionless approach has been attempted to predict the fluid entrainment. From an analysis of the system, the entrainment rate is influenced by the motive fluid velocity at the nozzle tip (U_{mn}), by the physical properties (ρ_m, μ_m, σ_m) and by the geometry of the ejector on one hand. On the other hand, it is influenced by the entrained gas velocity at the entrance to the suction chamber (U_{e0}), by the physical properties (ρ_e, μ_e) and by the pressure difference (ΔP) between the exit of the parallel diffuser and the entrance to the suction chamber.

If an *a* dimensional analysis relating the different variables exists, the entrainment rate can be expressed by the following two functions:

$$G = f_1(U_{mn}, \rho_m, \mu_m, \sigma_m, d_n, d_{sc}, g) \quad [9]$$

$$G = f_2(U_{e0}, \rho_e, \mu_e, d_0, \Delta P) \quad [10]$$

Solving [9] and [10] as mentioned earlier (Davies *et al.* 1967), we get:

$$\mathrm{Mr} = K_1\left(\frac{\rho_m U_{mn} d_n}{\mu_m}\right)^b\left(\frac{g\mu_m^{\ 4}}{\rho_m \sigma_m^{\ 3}}\right)^c(\mathrm{Ar})^j\left(\frac{\rho_e U_{e0} d_0}{\mu_e}\right)^f\left(\frac{\Delta P}{\rho_e U_{e0}^2}\right)^h \quad [11]$$

This work was conducted with a single nozzle, therefore Ar is constant (Ar = 4). Since the motive and entrained fluid Reynolds numbers are interrelated (figure 8), and the gas Reynolds number gives a linear relation with the Euler number in a log–log plot (figure 9), [11] can be simplified:

$$\mathrm{Mr} = K_2\left(\frac{\Delta P}{\rho_e U_{e0}^2}\right)^\alpha\left(\frac{g\mu_m^{\ 4}}{\rho_m \sigma_m^{\ 3}}\right)^\beta$$

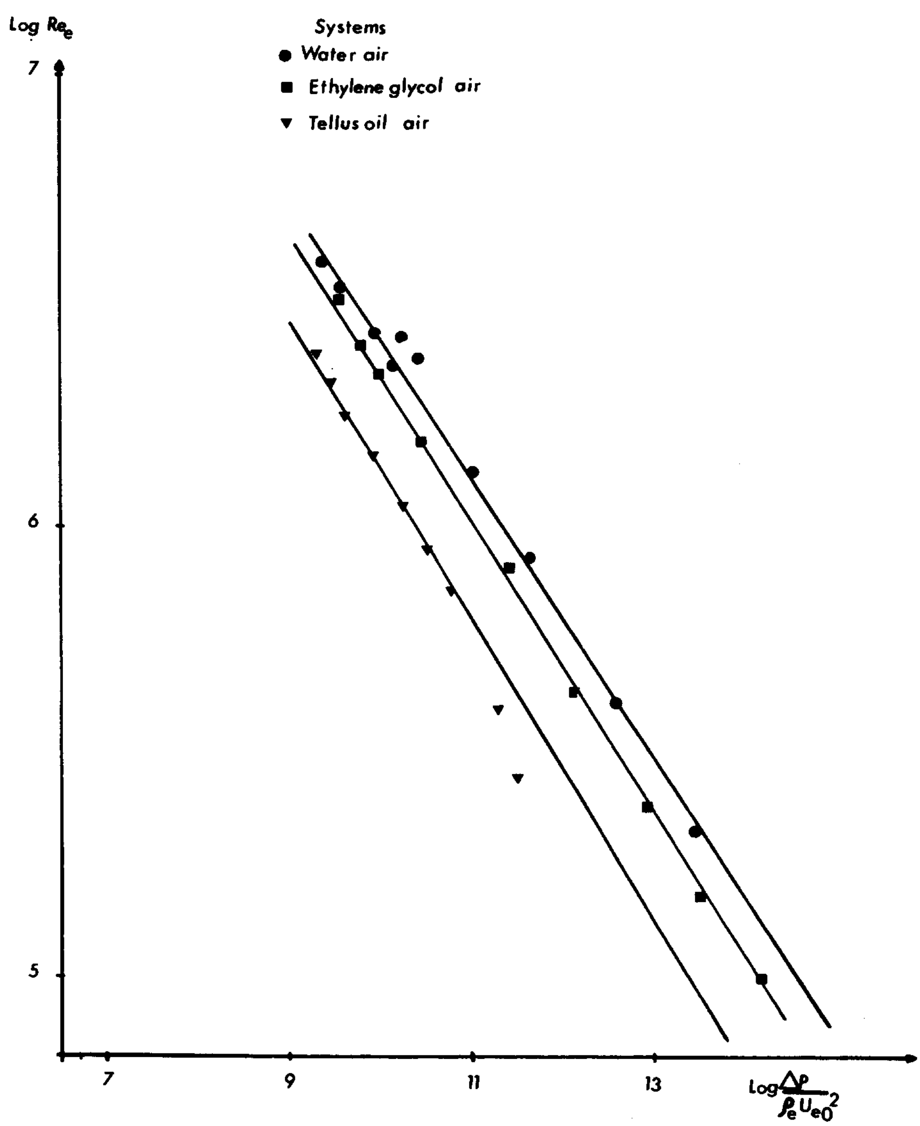

Figure 8. Relation between $[(d_0 U_{e0} \rho_e)/\mu_e]$ and $[(\Delta P)/\rho_e U_{e0}^2]$ for different liquid air systems.

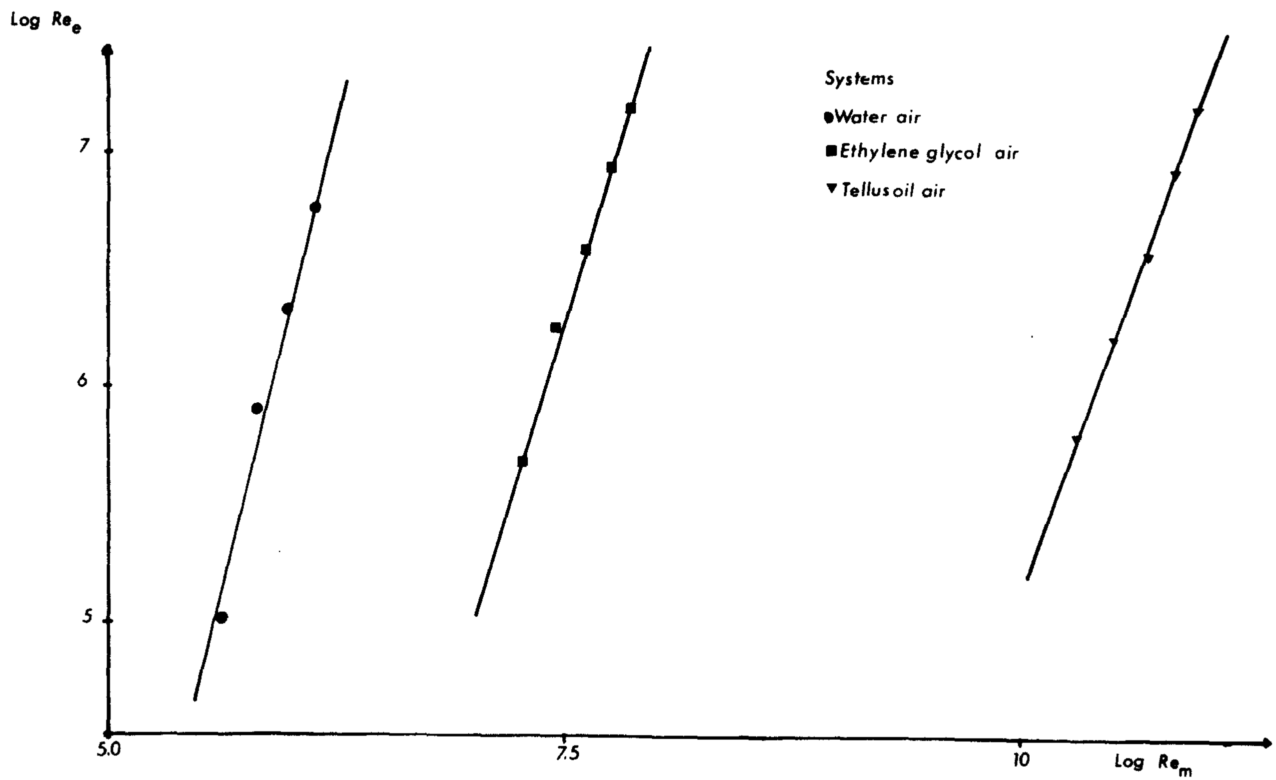

Figure 9. Relation between $[(d_n U_{e0} \rho_m)/\mu_m]$ and $[(\Delta P)/\rho_e U_{e0}^2]$ for different liquid air systems.

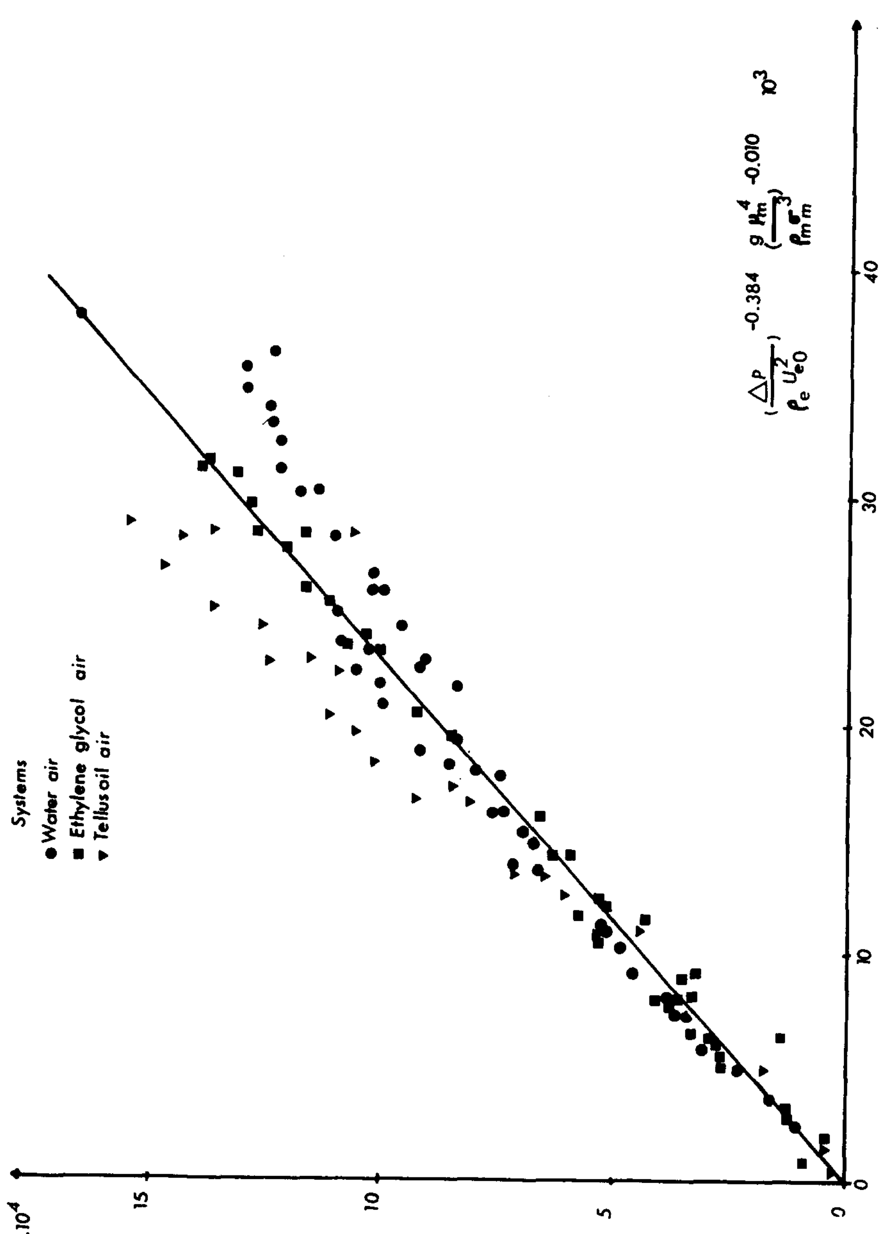

Figure 10. Correlation for gas–liquid vertical ejector.

From experimental data, the values of the exponents α and β have been evaluated by modified Gauss identification method (Joulia 1981). The final correlation shown in figure 9 may be expressed as:

$$\mathrm{Mr} = 43.86 \times 10^{-3}\left(\frac{\Delta P}{\rho_e U_{e0}^2}\right)^{-0.38}\left(\frac{g\mu_m{}^4}{\rho_m \sigma_m{}^3}\right)^{-0.01} \quad [12]$$

only available for $\mathrm{Ar} = 4$.

A comparison between experimental and calculated values of Mr obtained from our correlation is presented in figure 10, where the coaxial and froth flow zones appear. In this last case of flow ($\mathrm{Mr} < 75 \times 10^{-5}$), the established expression leads to good estimated values; for higher values of Mr, we note a slight change, probably in relation with the jet instability depending on physical properties. It leads to a good fitting for air–ethylene glycol system, but underestimates the results for the air–water system and overestimates these corresponding to the last system (air–Tellus oil).

6. REMARKS AND CONCLUSION

Taking into account the correlation proposed, it is possible to extend its application to other gases and liquids having different physical properties (ρ_m, σ_m and μ_m).

This work lets us compare the behaviour of the ejector for upward and downward flow, producing the same expression of K'' with β' or β''.

The possibility of an ejector to suck gas at pressure lower than the back pressure confirms that good absorption conditions are realized inside the contactor. A study for suction pressure (P_0) varying from $1.5 \times 10^5\,\mathrm{N/m^2}$ to $3 \times 10^5\,\mathrm{N/m^2}$ has been made at conditions of gas suction ($P_3 \gtrsim P_0$). The following points have been noticed:

—only a bubble flow has been observed;

—the sucked gas flowrates V'_{e0} at a pressure P'_0 higher than $10^5\,\mathrm{N/m^2}$ could be directed predicted from the sucked gas flowrates at atmospheric pressure noted P_0, V_{e0} by a relation such as:

$$V'_{e0} = V_{e0}\left(\frac{P'_0}{P_0}\right)^{0.5}.$$

Some studies of absorbed gas should permit the introduction in the established correlation a term taking into account a state change which involves a rise of Mr. Attempts are being made to introduce, a correction factor which allows the theory to be applied to ejectors and different geometries and also allows for gas absorption effects.

NOMENCLATURE

Ar area ratio, i.e. ratio of the area of the diffuser throat to the nozzle, dimensionless

Ar′ area ratio, i.e. ratio of the area of section at Plane 2 to that at Plane 1, dimensionless

a area of cross section as denoted by subscript, $\mathrm{m^2}$

b, c, j, f, h exponents in [10]

d diameter as denoted by subscript, m

E_1, E_2 energy losses by unit of volume due to expansion and gas–liquid mixing, $\mathrm{kg/m\,s^2}$

E'_2 energy losses, $\mathrm{kg\,m^2/s^2}$

F_1 force of gas–liquid mixing on solid surface, N

Fr Froude number, dimensionless

h height of the contactor, m
K'' overall loss factor
Mr mass ratio, i.e. ratio of mass flow rate of the entrained fluid to the motive fluid, dimensionless
G mass flow rate of entrained gas, kg/s
n moles of air, moles
ΔP $(P_3 - P_0)$, N/m^2
P, P' absolute pressure as denoted by subscript, N/m^2
R perfect gas constant, kg m^2/sec^2 g mole °K
Re Reynolds number, dimensionless
T ambient temperature (°K)
L mass flow rate of motive fluid (kg/s)
V, V' volume rate of flow as denoted by subscript, m^3/s
U, U' velocity of fluid and mixed fluid as denoted by subscript, m/s

Greek symbols

α, β exponents in [11]
β' kinetic pressure recovery factor $= \dfrac{P_3 - P_0 \dfrac{a_1}{a_2}}{\dfrac{1}{2}\rho_m U_{mn}^2}$
β'' kinetic pressure recovery factor $= \dfrac{(P_3 - P_0)}{\dfrac{1}{2}\rho_m U_{mn}^2}$
γ ratio of the area of the diffuser throat to secondary inlet, dimensionless
μ viscosity of fluid as denoted by subscript, kg/m s
ρ, ρ' density of fluid and mixed fluid as denoted by subscript, kg/m^3
ρ_r ratio of the densities of entrained and motive fluids, demensionless
σ surface tension as denoted by subscript, N/m

Subscripts

0, 1, 2, 3 at section 0, 1, 2, 3
e entrained fluid
m motive fluid
mn at nozzle tip
n at nozzle
sc at diffuser throat
s separator

REFERENCES

ACHARJEE, D. K., BHAT, P. A., MITRA A. K. & ROY, A. N. 1975 Studies on momentum transfer in vertical liquid-jet ejectors. *Ind. J. Technol.* **13**, 205–210.

BHAT, P. A., MITRA, A. K. & ROY, A. N. 1972 Momentum transfer in a horizontal liquid-jet ejector. *Can. J. Chem. Engng* **50**, 313–317.

BONNINGTON, S. T. 1964 A guide to jet pump design. *Br. Chem. Engng* **9**, 150–154.

BIRD, R. B., STEWART, W. E. & LIGHTFOOT, E. N. 1960 *Transport Phenomena*, pp. 210–217. Wiley International Edn, New York.

DAVIES, G. S., MITRA, A. K. & ROY, A. N. 1967 Momentum transfer studies in ejectors. *Ind. Engng Chem. Proc. Des. Dev.* **6**, 293–299.

HARRIS, L. S. 1966 Fume scrubbing with the ejector ventury system. *Chem. Engng Prog.* **62**, 55–59.

JOULIA, X. 1981 Contribution au développement d'un programme général de simulation (PSIGC). Application à l'analyse du fonctionnement d'un atelier de production d'acide nitrique. Thèse de Docteur Ingénieur, Toulouse, France.

LAURENT, A., FONTEIX, C. & CHARPENTIER, J. C. 1980 Simulation of a pilot scale liquid motivated, venturi jet scrubber by a laboratory scale model. *A.I.Ch.E. J.* **26**, 282–287.

PHELPS, A. H. 1966 What doesn't go up must down. *Chem. Engng Prog.* **62**, 37–40.

SHAH, I. S. 1968 Pulp plant: pollution control. *Chem. Engng Prog.* **64**, 66–67.

WITTE, J. H. 1965 Efficiency and design of liquid gas ejectors. *Br. Chem. Engng* **10**, 602–607.